

From the microscopic to the macroscopic world: from nucleons to neutron stars

Gandolfi, S.

Theoretical Division, Los Alamos National Laboratory, Los Alamos, New Mexico
87545, USA

Lippuner, J.

Computational Physics and Methods, CCS-2, Los Alamos National Laboratory, Los
Alamos, New Mexico 87545, USA
Center for Theoretical Astrophysics, Los Alamos National Laboratory, Los Alamos,
NM 87545, USA

Steiner, A. W.

Department of Physics and Astronomy, University of Tennessee, Knoxville, TN
37996, USA
Physics Division, Oak Ridge National Laboratory, Oak Ridge, TN 37831, USA

Tews, I.

Theoretical Division, Los Alamos National Laboratory, Los Alamos, New Mexico
87545, USA

Du, X.

Department of Physics and Astronomy, University of Tennessee, Knoxville, TN
37996, USA

Al-Mamun, M.

Department of Physics and Astronomy, University of Tennessee, Knoxville, TN
37996, USA

Abstract. Recent observations of neutron-star properties, in particular the recent detection of gravitational waves emitted from binary neutron stars, GW 170817, open the way to put strong constraints on nuclear interactions. In this paper, we review the state of the art in calculating the equation of state of strongly interacting matter from first principle calculations starting from microscopic interactions among nucleons. We then review selected properties of neutron stars that can be directly compared with present and future observations.

1. Introduction:

The idea that astronomical observations may provide insight into nuclear interactions originated in the 1950s [1, 2]. There have been a few landmark neutron-star observations in the past decade which can be directly connected to the interaction between nucleons. Two neutron-star mass measurements obtain results ~ 2 solar masses [3, 4] (see also [5]). Simultaneous information on neutron-star masses and radii is becoming available [6, 7] (see updates in Refs. [8, 9, 10]). Finally, the first detection of gravitational waves from a binary neutron-star merger, GW 170817, has also provided mass and tidal deformability constraints [11], and its electromagnetic counterpart has demonstrated that neutron-star mergers are an important source for r-process nuclei. These advances in neutron-star observations provide a unique opportunity to improve our knowledge of nuclear physics. Although the corresponding length scales are separated by many orders of magnitude, properties of neutron stars and nuclei are strongly connected. In particular, the equation of state (EOS) of the crust and the outer core is one of the main ingredients for neutron-star structure, determining radii, tidal deformabilities, and other properties of neutron stars. The EOS is obviously related to nuclear forces and properties of nuclei.

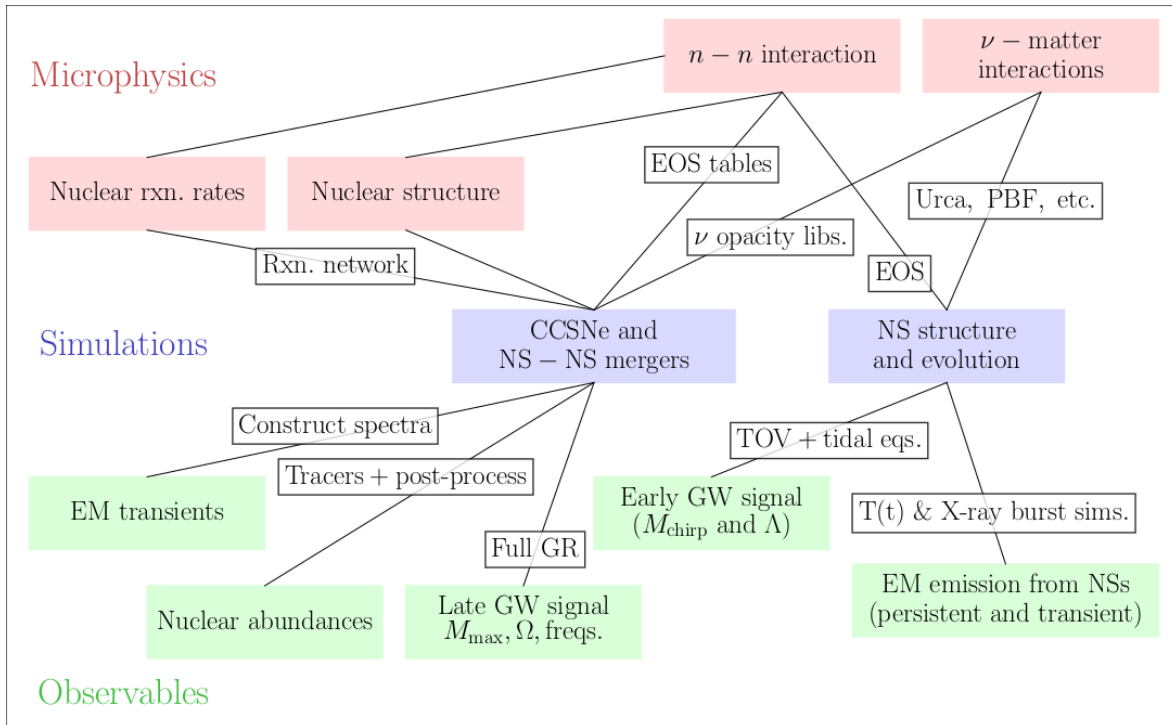


Figure 1. A diagram representing the connections between microphysical models and astrophysical observations.

At the femtometer scale, it is of fundamental importance to understand how nucleons interact, how neutrinos interact in nuclear matter, how nuclei are formed and how their properties emerge. All these are among the main ingredients for astrophysical

simulations, including simulations of supernova explosions and the evolution of neutron stars. Those simulations predict or explain observations of phenomena which can have exiameter (100 light-year) length scales, including electromagnetic and gravitational-wave emission, nuclear abundances, ejecta from binary neutron-star mergers, and others; see Fig. 1 for a diagram summarizing the connections between microphysical models, simulations, and observations. There is a strong connection between the microscopic and macroscopic world, separated by many orders of magnitude. Information in Fig. 1 flows both ways: microphysical models can be used to describe observations, and observations constrain our knowledge of nuclear interactions, nuclear structure, and nuclear reactions.

In this paper, we will start by briefly discussing how nuclear forces are constructed and tested, how they are used to calculate the EOS, and then how the EOS is used to predict selected properties of neutron stars. We will then provide details regarding how Bayesian inference can be utilized to attack the “inverse problem”: the problem of constraining our model parameters from observational data.

2. The EOS

Most of the static and dynamical properties of neutron stars can be calculated once an Equation of State (EOS) describing the matter inside the stars is specified. At very low densities, in the outer crust of neutron stars, the matter is mainly composed of a lattice of ordinary nuclei in the iron region. With increasing density, the neutron chemical potential also increases and nuclei become extremely neutron-rich. At the interface with the inner crust, the neutron chemical potential is sufficiently high so that neutrons start to drip out of the nuclei, and the nuclei start to be surrounded by a sea of neutrons. Eventually, at the bottom of the inner crust, the geometry of nuclei begins to be deformed, forming the so-called “pasta” phase. At about half the saturation density, $\rho_0 = 0.16 \text{ fm}^{-3} \approx 2.7 \cdot 10^{14} \text{ g/cm}^3$, the nuclei completely melt, and the neutron-star core begins. Here, matter is composed of a uniform liquid of a large fraction of neutrons with a few protons, electrons, and eventually muons. At even higher densities, above $\approx 2\rho_0$, the composition of matter is basically unknown. In this inner core of the neutron star, many scenarios for the state of matter have been suggested, for example the formation of hyperons [12], quark matter [13], or other more exotic condensates. Fig. 2 shows the nature of these layers and gives a summary of properties of a typical neutron star.

The full description of the EOS in the whole range of densities encountered inside a neutron star, i.e. up to several times nuclear saturation density, is a formidable task. Especially for the inner core, most EOS used in astrophysical simulations necessarily make some model-dependent assumptions. However, once an EOS $\epsilon(p)$ is specified, the mass-radius relation of a non-rotating neutron star can be easily calculated by solving the Tolman-Oppenheimer-Volkoff (TOV) equations:

$$\frac{dP}{dr} = -\frac{G[m(r) + 4\pi r^3 P/c^2][\epsilon + P/c^2]}{r[r - 2Gm(r)/c^2]},$$

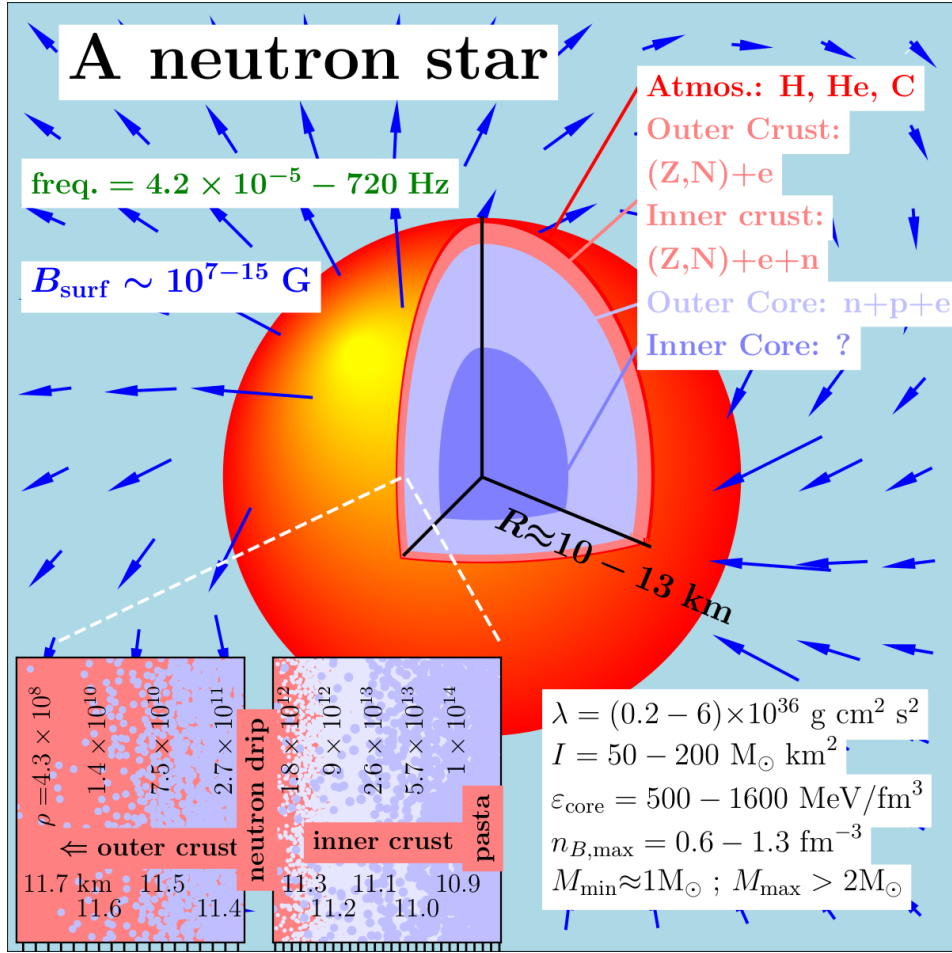


Figure 2. A summary of the microphysics of neutron stars. In the upper left of the figure, the observational limits on rotation frequency [14, 15] and the magnetic field [16, 17] are given. The upper right panel shows the composition of the various layers. The lower left shows a schematic representation of the crust, where the dark blue color represents nuclei and the light blue color represents free neutrons. The limits on radius from X-ray observations are shown near the center [18]. Limits on the tidal deformability, moment of inertia, energy density in the core, and baryon density in the core [19] are shown in the lower right panel. This figure was inspired by a previous version by Dany Page available at <http://www.astroscu.unam.mx/neutrones/NS-Picture/NStar/NStar.html>.

$$\frac{dm(r)}{dr} = 4\pi\epsilon r^2, \quad (1)$$

where P and ϵ are the pressure and the energy density (including the rest mass energy density contribution), $m(r)$ is the gravitational mass enclosed within a radius r , and G is the gravitational constant. The solution of the TOV equations for a given central density gives the profiles of $\rho(r)$, $\epsilon(r)$ and $P(r)$ as functions of radius r , and also the total radius R and mass $M = m(R)$, specified by the condition $P(R) = 0$. By varying the input central density, the mass-radius (MR) relation is mapped out. The resulting MR relation is in one-to-one correspondence with the input EOS (as summarized in

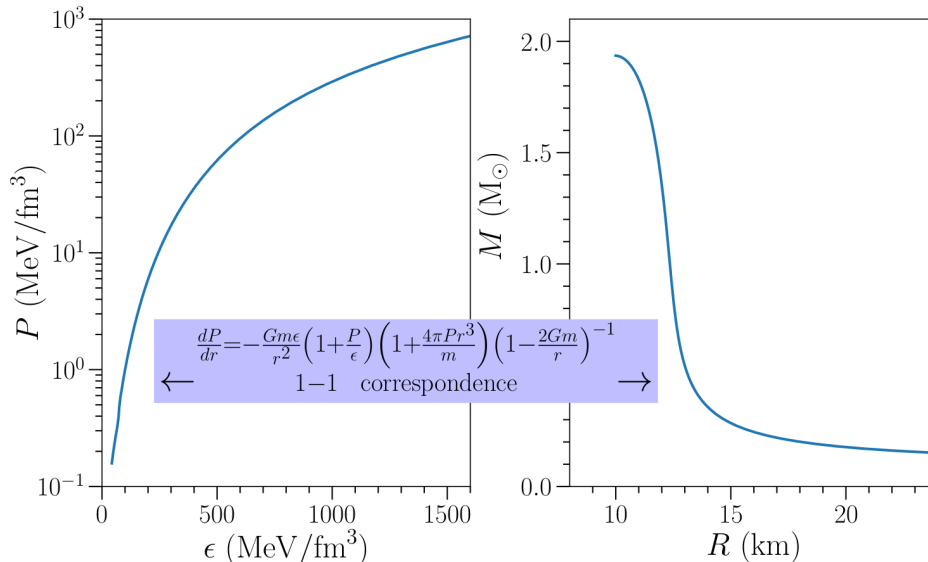


Figure 3. The EOS and MR curve of Skyrme model NRAPR [20].

Fig. 3), which offers the possibility to measure the EOS, and thus the properties of strongly interacting matter up to a few times saturation density, by mapping out the MR relation observationally. In addition to properties of isolated neutron stars, also other dynamical properties of neutron stars and binary neutron-star mergers depend on the EOS, including the gravitational-wave spectrum, the amount of ejected material, and others.

An ideal starting point for the EOS of neutron-star matter is the EOS of pure neutron matter (PNM), which is a homogeneous system that contains only neutrons. The EOS of PNM can be calculated using sophisticated many-body methods once a nuclear Hamiltonian is specified. Among other methods, these include variational methods based on the cluster expansion [21], many-body perturbation theory [22], the coupled-cluster method [23], and Quantum Monte Carlo methods [24, 25]. In this paper, we will focus on recent results obtained with the Auxiliary Field Diffusion Monte Carlo (AFDMC) method, which was originally introduced by Schmidt and Fantoni [26], and is ideally suited to study neutron matter [27, 28].

The main idea of QMC methods is to evolve a many-body wave function in imaginary-time:

$$\Psi(\tau) = \exp[-H\tau] \Psi_v, \quad (2)$$

where Ψ_v is a variational ansatz of the many-body wave function and H is the Hamiltonian describing the system. In the limit of $\tau \rightarrow \infty$, Ψ approaches the ground-state of H . The evolution in imaginary-time is performed by sampling configurations of the system using Monte Carlo techniques, and expectation values are evaluated over the sampled configurations. For more details see for example Refs. [28, 29, 30, 31, 32, 33].

In addition to the many-body method, one needs the nuclear Hamiltonian as input,

which describes the interactions among nucleons. In AFDMC, nuclei and neutron matter are described by non-relativistic point-like particles interacting via two- and three-body forces:

$$H_{\text{nuc}} = \sum_i \frac{p_i^2}{2m_N} + \sum_{i<j} v_{ij} + \sum_{i<j<k} v_{ijk}. \quad (3)$$

The first two-body potential that has been extensively used with the AFDMC method is the phenomenological Argonne AV8' potential [34], that is a simplified form of the Argonne AV18 potential [35]. Although simpler to use in QMC calculations, the AV8' potential provides almost the same accuracy as AV18 in fitting NN scattering data. In addition to such two-body potentials, it was shown that one has to include also a three-body interaction to being able to describe nuclear systems accurately, e.g., to correctly describe the binding energy of light nuclei [28]. However, the three-body force is not as well constrained as the NN interaction. The Urbana IX (UIX) three-body force has been originally proposed to be used in combination with the Argonne AV18 and AV8' [36] potentials. Although it slightly underbinds the energy of light nuclei, it has been extensively used to study the equation of state of nuclear and neutron matter [21, 30, 37]. The AV8'+UIX Hamiltonian has been used in many works, and provided a fairly good description of neutron star properties [37].

However, such phenomenological interactions suffer from certain shortcomings. Most importantly, they do not enable to estimate reliable theoretical uncertainties and cannot be systematically improved. These shortcomings can be addressed with the advent of chiral effective field theory (EFT), which offers a systematic expansion of nuclear forces that allows for theoretical uncertainties [38, 39].

In this approach, the relevant degrees of freedom are nucleons that can interact via explicit pion exchanges or via short-range contact interactions. The relevant diagrams entering in the nucleon-nucleon interaction are systematically organized in powers of p/Λ_b , where p is the typical momenta of nucleons in the given nuclear system, i.e. similar to the pion mass $m_\pi \approx 140$ MeV, and $\Lambda_b \approx 500 - 600$ MeV [40] is the so-called breakdown scale, where the chiral EFT expansion is expected to lose its validity due to the increasing importance of shorter-range physics, i.e., new degrees of freedom. Chiral interactions include long-range pion-exchange physics explicitly, while short-range physics is described by a general operator basis consistent with all symmetries of the fundamental theory, Quantum Chromodynamics. The long-range pion-exchange terms entering into the chiral EFT potentials are fully determined by π -nucleon scattering data, while the parameters associated to the contact terms, called low-energy constants (LECs), are typically constrained by fitting nucleon-nucleon scattering data. For more details see Ref. [38]. Hamiltonians from chiral EFT have been recently combined with QMC methods [41, 42, 43, 44, 31], and give very reasonable predictions of properties of nuclei up to $A=16$, including energies, radii, and momentum distributions, and neutron- α scattering.

In addition, these interactions give a reasonable description of PNM [43, 45]. We show the PNM EOS calculated using AFDMC with local chiral interactions and the

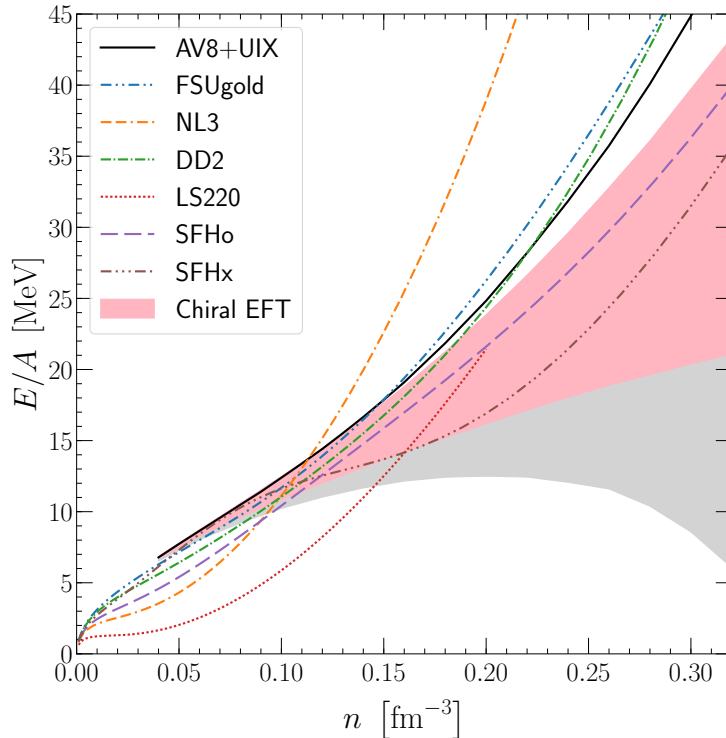


Figure 4. The EOS of pure neutron matter calculated using the AFDMC method with local chiral interactions with a cutoff of $R_0 = 1.0$ fm (red and gray bands), and using the AV8'+UIX Hamiltonian (black solid line). We also compare the AFDMC results with several EOS that are typically used in astrophysical simulations. See the text for more details.

AV8'+UIX interaction in Fig. 4. The red and gray bands represent AFDMC results using three different parametrizations of the three-body force constrained in light nuclei, although they give different results in pure neutron matter due to regulator artifacts; see Ref. [43] for more details. In particular, one of them gives negative pressure in pure neutron matter between $1 - 2\rho_0$, and is represented by the gray band in Fig. 4. The other two parametrization give instead the red band in the figure, and can be employed to describe neutron stars [45].

The AFDMC results are compared to other models that are commonly used in astrophysical simulations: the Lattimer-Swesty EOS with incompressibility 220 [46], the TM1, SFHo, and SFHx EOSs [47], the FSU and NL3 EOSs [48], and the DD2 EOS [49]. We find that AFDMC calculations put strong constraints on the EOS of pure neutron matter.

The AFDMC results for the EOS of PNM can be conveniently parametrized using the functional

$$E_{PNM}(\rho) = a \left(\frac{\rho}{\rho_0} \right)^\alpha + b \left(\frac{\rho}{\rho_0} \right)^\beta, \quad (4)$$

that represents the energy per particle (without the rest mass energy) as a function of

neutron density. We can define the symmetry energy as

$$E_{\text{sym}}(\rho) = E_{\text{PNM}}(\rho) - E_{\text{SNM}}(\rho), \quad (5)$$

where $E_{\text{SNM}}(\rho)$ is the EOS of symmetric nuclear matter, which is not known. However, by requiring that symmetric nuclear matter saturates at an energy $E_{\text{SNM}}(\rho_0) = -16$ MeV, and using the expression for $E_{\text{PNM}}(\rho)$ above, the symmetry energy and slope can be obtained by

$$\begin{aligned} E_{\text{sym}} &= a + b + 16, \\ L &= 3(a\alpha + b\beta). \end{aligned} \quad (6)$$

Thus, for $E_{\text{SNM}}(\rho)$ we find

$$E_{\text{SNM}}(\rho) = E_{\text{PNM}}(\rho) - E_{\text{sym}}(\rho). \quad (7)$$

Assuming a quadratic expansion in the proton fraction $x = \rho_p/\rho$, the EOS at a finite proton fraction is given by

$$\begin{aligned} E(\rho, x) &= E_{\text{SNM}}(\rho) + E_{\text{sym}}(\rho)(1 - 2x)^2 = \\ &= E_{\text{PNM}}(\rho) + E_{\text{sym}}(\rho) [(1 - 2x)^2 - 1]. \end{aligned} \quad (8)$$

The latter equation gives the expected results for pure neutron matter ($x = 0$) and symmetric nuclear matter ($x = 1/2$).

A very common parametrization for the symmetry energy is given by

$$E_{\text{sym}}(\rho) = C \left(\frac{\rho}{\rho_0} \right)^\gamma, \quad (9)$$

and using this definition, the slope parameter L is linear with $C = E_{\text{sym}}(\rho_0)$:

$$L = 3\rho_0 \frac{\partial E_{\text{sym}}(\rho)}{\partial \rho} = 3\rho_0 \frac{C\gamma}{\rho} \left(\frac{\rho}{\rho_0} \right)^\gamma \rightarrow L \sim C. \quad (10)$$

From Eq. (6), we can obtain C :

$$C = a + b + 16. \quad (11)$$

We can put an additional constraint on our simple ansatz by requiring that the pressure of SNM is zero at saturation, i.e.,

$$P = \rho^2 \frac{\partial E_{\text{SNM}}}{\partial \rho} \Big|_{\rho=\rho_0} = 0. \quad (12)$$

This leads to the condition

$$\gamma = \frac{a\alpha + b\beta}{C} = \frac{a\alpha + b\beta}{16 + a + b}. \quad (13)$$

Note that by combining equations, we also find

$$L = 3(a\alpha + b\beta). \quad (14)$$

With these simple assumptions, the general form of the EOS as a function of density and proton fraction becomes:

$$E(\rho, x) = E_{\text{PNM}}(\rho) + (16 + a + b) \left(\frac{\rho}{\rho_0} \right)^{\frac{a\alpha + b\beta}{16 + a + b}} [(1 - 2x)^2 - 1]. \quad (15)$$

Hamiltonian	E_{sym} (MeV)	L (MeV)	a (MeV)	α	b (MeV)	β
AV8'	30.5	31.3	12.7	0.49	1.78	2.26
AV8'+UIX	35.1	63.6	13.4	0.514	5.62	2.436
N ² LO ^{up} (1.0 fm)	34.8	56.2	13.19	0.51	5.66	2.12
N ² LO ^{low} (1.0 fm)	30.2	24.4	13.87	0.59	0.36	-0.05
N ² LO ^{mid} (1.0 fm)	32.5	40.5	13.13	0.51	3.41	1.99

Table 1. Fitting parameters for the neutron matter EOS defined above. The values of E_{sym} and L are obtained by fitting the AFDMC results. The N²LO parameter represent the higher, middle and lower part of the read band of Fig. 4.

The parametrizations for selected EOSs are reported in Table 1, together with the corresponding symmetry energy and its slope.

While L is now strongly constrained by chiral EFT and QMC, these constraints complement those from X-ray observations of neutron stars. Ref. [50] found $43 < L < 52$ MeV to within 68% confidence based on an analysis of neutron-star observations using Eq. 4.

3. Neutron star properties

As described above, once the EOS is specified it is easy to calculate the mass-radius relation of a neutron star. However, since the neutron star does not consist of pure neutron matter, one has to find ways of extending the microscopic PNM calculations to neutron-star conditions. In the following, we will discuss a few possibilities.

3.1. Effect of leptons

Typical neutron-star properties can be calculated directly from the PNM EOS, but such an approach misses the effects of the neutron-star crust and the remaining protons. Therefore, a more realistic EOS should contain these effects which can be estimated from the PNM EOS.

By starting from Eq. 15 we can solve for $x(\rho)$ by imposing β -equilibrium between neutrons, protons, electrons, and muons. With

$$\begin{aligned} \epsilon &= \rho [E(\rho, x) + m_n(1 - x) + m_p(x)], \\ \mu_y &= \frac{\partial(\rho E)}{\partial \rho_y}, \end{aligned} \quad (16)$$

where ϵ is the total energy density, m_n is the neutron mass, m_p is the proton mass, and μ_y the chemical potential with $y = n, p$. We can easily obtain

$$\mu_n - \mu_p = 4(1 - 2x)E_{\text{sym}}(\rho). \quad (17)$$

Charge neutrality requires that

$$\mu_n - \mu_p = \mu_e = \mu_\mu \quad (18)$$

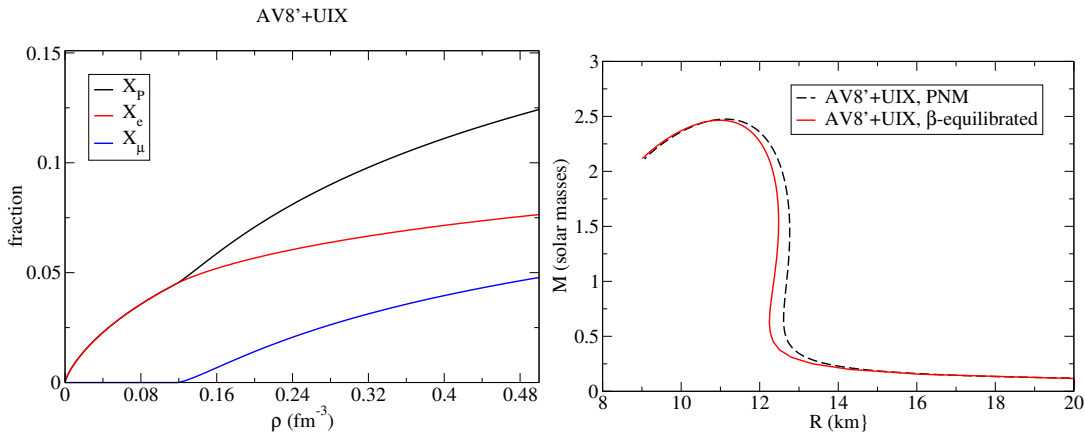


Figure 5. Left panel: proton and lepton fractions obtained from the AFDMC EOS. Right panel: neutron star structure for pure neutron and β -equilibrated matter.

We take electrons to be relativistic and degenerate:

$$\mu_e = (m_e^2 + \hbar^2 k_F^2)^{1/2} \approx \hbar(3\pi^2 \rho x_e)^{1/3}, \quad (19)$$

and for the muons

$$\mu_\mu = [m_\mu^2 + \hbar^2(3\pi^2 \rho x_\mu)^{2/3}]^{1/2}. \quad (20)$$

We then calculate all the fractions by imposing the charge neutrality, chemical potential as above, and

$$x = x_e + x_\mu. \quad (21)$$

Homogeneous matter in β -equilibrium is a valid model for sufficiently high densities, where nuclei are not present. Therefore, the AFDMC EOS is used for $\rho \geq \rho_{\text{crust}} = 0.08 \text{ fm}^{-3}$. For the low-density EOS, describing the crust of a neutron star, results of earlier works can be used; see e.g. Ref. [51] and [52]. For the AV8'+UIX EOS, we show the MR relations for the PNM EOS and when we assume β equilibrium in Fig 5, where also the proton and lepton fractions are presented. We can see that the effect of protons is giving a small correction to the neutron-star radius given the current uncertainties in neutron-star observations [50].

3.2. High-density extrapolations

The approach in the previous section assumes a description in terms of nucleons and leptons to be valid in the whole neutron star. However, while this assumption might be true, the EOS might also explore more extreme density behavior at higher densities, as produced by, e.g., strong phase transitions to exotic forms of matter.

To being able to analyze neutron-star properties, general extrapolations schemes have to be used which are constrained by nuclear-physics input at low densities as well as observational constraints. Such general extrapolation schemes can be based on piecewise polytropes, where polytropes are line segments in $(\log \epsilon, \log P)$ space; see

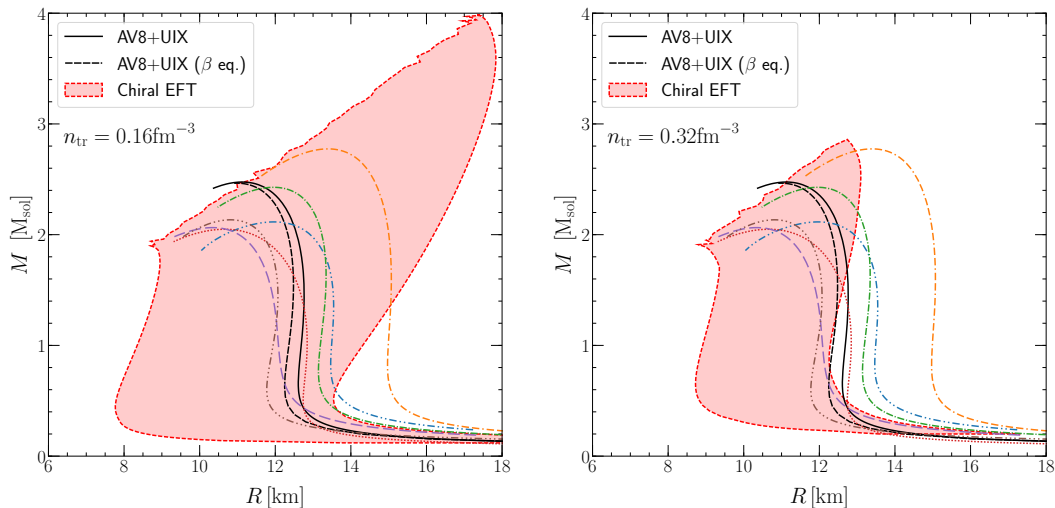


Figure 6. General MR extrapolation using the chiral EFT PNM EOS of Fig. 4 up to saturation density (left) or up to two times saturation density (right). We compare with results for the same model EOS as in Fig. 4.

e.g., Refs. [53, 7, 54]. However, Ref. [55] showed that line segments in (ϵ, P) space can more easily represent models which have a phase transition to exotic matter in the neutron-star core.

In contrast, in Refs. [56, 57] another general extrapolation scheme starting from the PNM EOS from chiral EFT was developed, that used the speed of sound, c_S in neutron stars. This scheme was based on the initial work of Refs. [58, 59], but represents an extension of these models by exploring all allowed parameter space for the speed of sound c_S , defined as

$$c_S = \sqrt{\frac{\partial p(\epsilon)}{\partial \epsilon}}. \quad (22)$$

In particular, models are constrained by the PNM EOS up to a certain density n_{tr} which is varied between 1-2 ρ_0 . This PNM EOS is extended to β -equilibrium and includes a crust as discussed in Ref. [60]. From the resulting neutron-star EOS, the speed of sound is computed up to n_{tr} . Beyond this density, many possible paths in the $c_S - n$ plane are explored by randomly sampling several points $c_S^2(n)$ between n_{tr} and 12 ρ_0 , and connecting them by linear segments. During this procedure, it is enforced that $0 \leq c_S \leq c$ and that the resulting EOSs are sufficiently stiff to support a two-solar-mass neutron star [3, 4]. For more details on this extrapolation scheme, see Ref. [61].

We show the resulting MR regions in Fig. 6, where we compare with the AV8'+UIX result from the previous section as well as the same model EOS of Fig. 4. We find that chiral EFT input can place strong constraints on the MR relation, ruling out too stiff model EOS, e.g., the NL3 parametrization. In particular, the density range between 1-2 ρ_0 is very important to reduce the uncertainty in the MR plane and improved calculations in this density range with smaller uncertainties will be useful to pin down

the MR relation of neutron stars.

4. Connecting the Microphysics with the Multi-messenger Observations

Multi-messenger astronomy requires a strong foundation of microphysics in order to fully interpret the observations. The first evidence of this fact was the observation of both photons and neutrinos from supernova 1987A. This observation confirmed the basic picture of stellar evolution, which required significant nuclear and neutrino physics input [e.g. 62, 63, 64, 65, 66, 67]. More recently, the first gravitational-wave observation of a binary neutron-star merger, GW170817, has further highlighted the tight connection between microphysics, including the nuclear EOS, and multi-messenger astronomy observations [e.g. 11, 68].

Neutron-star mergers have long been thought to be the progenitors of short gamma-ray bursts (GRBs) and a significant, if not dominant, site of r-process nucleosynthesis [e.g. 69, 70, 71, 72, 73, 74, 75, 76, 77]. This basic picture was confirmed by GW170817, which was observed in coincidence with a short GRB (GRB170817A) from the same location in the sky [e.g. 78, 79, 80]. Subsequent followup observations with instruments and telescopes spanning the entire electro-magnetic spectrum revealed a kilonova [e.g. 78, 81, 82, 83, 84, 85]. Kilonovae are rapidly fading (timescale of a few weeks) optical and infrared transients that are powered by the radioactive decay of the newly synthesized r-process elements [e.g. 86, 87, 88, 89, 90]. They are the smoking gun signatures of r-process nucleosynthesis events.

Even though GW170817 confirmed some aspects of the basic picture of neutron-star mergers and the role they play in r-process nucleosynthesis, many details remain unresolved. Over the coming years, LIGO/VIRGO will observe more neutron-star mergers and we should be able to find the associated kilonovae for at least some of them [e.g. 93, 94, 95, 96, 97]. A detailed understanding of the microphysics will be crucial in accurately modelling the rich multi-messenger observational data from these events to fully understand them and extract system parameters that are not directly observable. Specifically, microphysics and the nuclear EOS directly impact the amount and possibly morphology of the mass ejecta and accretion disk [e.g. 98, 99, 100, 101, 102, 103, 104, 105, 68, 106, 107] that forms around the compact central remnant. They also determine how long a hypermassive neutron star (HMNS) could live, if one forms, and this lifetime affects the amount of ejecta blown away from the disk and its neutron-richness, which in turn determines what elements the r-process can synthesize [e.g. 108, 92]. An example of the effect of the lifetime of the HMNS is shown in Fig. 7. Neutrino interactions in general are very important to determine the composition of the ejecta and subsequent nucleosynthesis [e.g. 109, 110, 111, 112, 113, 114, 115, 116]. All of these properties affected by microphysics directly influence the kilonova lightcurve, nucleosynthetic yields, and possibly the gravitational wave signal. Therefore, we need to get the microphysics right in order to draw meaningful conclusions from neutron-star merger and kilonova observations about their intrinsic properties and how they enrich

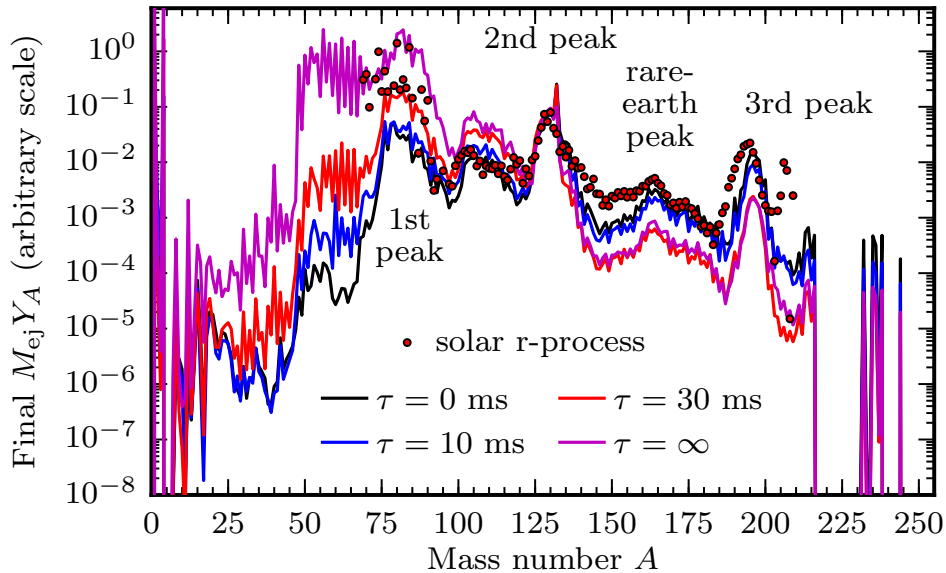


Figure 7. Final abundances times the total ejecta mass M_{ej} of accretion disk outflows around a hypermassive neutron star (HMNS) for different lifetimes τ of the HMNS. If the HMNS collapses to a black hole within 10 ms, the resulting nucleosynthesis pattern matches the solar pattern quite well. But if the lifetime is $\tau \gtrsim 30$ ms (including if the HMNS never collapses), the rare-earth and 3rd r-process peaks are suppressed with respect to the solar pattern. The dots show the solar r-process pattern from [91]. This is an adapted version of Fig. 4 in [92], see that reference for details.

the galaxy with heavy elements [e.g. 117].

4.1. Constraining the Microphysics of Merger Simulations with GW170817

Neutron-star merger simulations require a three-dimensional EOS table: a description of several thermodynamic quantities as a function of the baryon density, ρ , electron fraction, Y_e , and the temperature, T . Until recently, only about a dozen of these EOS tables was available. These EOS tables explore only a tiny fraction of the large space of EOSs which appear to be compatible with our current knowledge of the nucleon-nucleon interaction. For a review, see Ref. [118].

This state of affairs changed when Ref. [119] released an open-source code for EOS tables built upon the Skyrme interaction. This code allows one to fully explore a large space of EOSs. In particular, a merger simulation may systematically probe the sensitivity of the observables generated by the merger simulation to the parameters in the Skyrme interaction. This code, however, is limited by the applicability of the Skyrme interaction.

In Ref. [120] we presented a new class of phenomenological EOS for homogeneous nucleonic matter. The EOS is constructed to simultaneously match (i) second order virial expansion coefficients from nucleon-nucleon scattering phase shifts at high temperature and low density, (ii) experimental results of nuclear mass and radii,

(iii) QMC calculations for neutron matter at saturation density, (iv) astrophysical observational measurements on neutrons star radii, (v) theoretical calculations with chiral perturbation field theory at finite temperature near the saturation density. It allows for computing the variation in the thermodynamic quantities based on the uncertainties of nuclear interaction.

Our free energy per particle can be written as

$$F_{\text{np}}(\rho, x, T) = F_{\text{virial}}(\rho, x, T)g + F_{\text{deg}}(\rho, x, T)(1 - g), \quad (23)$$

where x is the number of protons per baryon (assumed here to be equal to Y_e), f_{virial} is the virial free energy contribution [121] and f_{deg} is the free energy for degenerate matter. The function is defined by

$$g = 1/(1 + 3z_n^2 + 3z_p^2), \quad (24)$$

where $z_i \equiv \exp(\mu_i/T)$ are the fugacities. Since the virial expansion is valid when $z_n^2, z_p^2 \ll 1$, this functional form gives $g \approx 1$, thus the dominant contribution is from F_{virial} . Otherwise, if z_n or z_p are large, $F_{\text{np}} \approx F_{\text{deg}}$. The free energy per particle of degenerate matter is further defined assuming quadratic expansion

$$F_{\text{deg}}(\rho, x, T) = F_{\text{Skyrme}}(\rho, x = 1/2, T = 0) + \delta^2 E_{\text{sym}}(\rho) + F_{\text{hot}}(\rho, x, T) - F_{\text{hot}}(\rho, x = 0, T) \quad (25)$$

with $\delta = 1 - 2x$. The 1000 parameter set of Skyrme model was chosen from UNEDF collaboration fitted to several nuclear mass, charge radii and pairing energies using Bayesian inference [122]. The F_{hot} is finite temperature results based on Kohn-Luttinger-Ward perturbation series fitted to Skyrme functional form [123, 124]. The symmetry energy is defined by

$$E_{\text{sym}} = h(\rho)E_{\text{PNM}} + [1 - h(\rho)]E_{\text{NS}}(\rho) - F_{\text{Skyrme}}(\rho, x = 1/2, T = 0), \quad (26)$$

where we interpolate between Eq. (4) near saturation density ρ_0 and a polynomial fit to neutron star observational data [7] above $2\rho_0$ using a function h , defined as

$$h = \frac{1}{1 + \exp[\gamma(\rho - 3/2\rho_0)]}, \quad (27)$$

where $\gamma = 20.0 \text{ fm}^3$. At zero temperature, the EOS can be compared to Eq. (15).

The advantage of the formalism above is that it allows us not only to compute the EOS of homogeneous nucleonic matter over the full range of densities, electron fractions, and temperatures, but it allows us to describe the probability distribution of the EOS. Formulating the EOS in this way allows us to easily determine the impact that observations might have on the EOS. This is demonstrated in Fig. 8 where the correlation between the free energy per baryon at $\rho = 3\rho_0$ and the tidal deformability of a $1.4 M_{\odot}$ neutron star is shown. The tidal polarizability describes how a neutron star deforms under an external gravitational field, as produced by a companion star. It is given by

$$\Lambda = \frac{2}{3}k_2 \left(\frac{c^2 R}{G M} \right)^5, \quad (28)$$

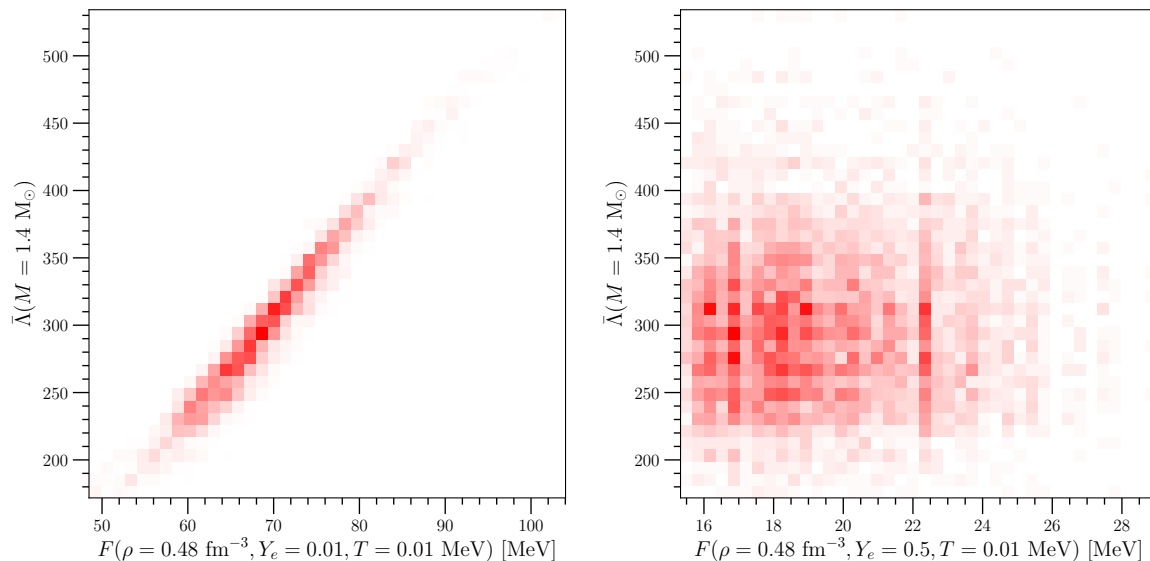


Figure 8. Two-dimensional histograms of the tidal deformability versus the free energy per particle from the DSH formalism [120] at $\rho = 0.48 \text{ fm}^{-3}$ in either neutron-rich matter (left panel) or isospin-symmetric matter (right panel). The distribution of tidal deformabilities already accounts for the constraints due to neutron-star mass and radius constraints from X-ray observations [19]. The left panel shows that a constraint on the tidal deformability has a strong impact on constraining the EOS of neutron-rich matter. However, the right panel shows that GW observations provide almost no constraint on the EOS of symmetric nuclear matter. This demonstrates the role of the nuclear symmetry at high densities: while neutron-star observations constrain neutron-rich matter, they do not constrain the symmetry energy at high densities unless one assumes that the EOS of nuclear matter is otherwise fixed.

with the tidal Love number k_2 which has to be solved together with the TOV equations; see, e.g., Ref. [125]. As is expected, the free energy of neutron-rich matter is strongly correlated with the tidal deformability, but the uncertainty in the free energy of isospin-symmetric matter is not impacted by constraints on the tidal deformability.

4.2. EOS constraints from tidal polarizabilities

The analysis of the gravitational-wave signal from the inspiral phase of two merging neutron stars allows to place constraints on properties of the binary system, e.g., the chirp mass or mass ratio, as well as on properties of individual neutron stars. For a neutron-star binary, the binary tidal polarizability can be defined as

$$\tilde{\Lambda} = \frac{16}{13} \left(\frac{(m_1 + 12m_2)m_1^4 \Lambda_1}{m_{\text{tot}}^5} + \frac{(m_2 + 12m_1)m_2^4 \Lambda_3}{m_{\text{tot}}^5} \right). \quad (29)$$

This quantity, $\tilde{\Lambda}$, can be constrained from the GW signal of a NS merger. For the first NS merger observed, GW170817, this tidal polarizability originally was constrained to be $\tilde{\Lambda} \leq 800$ at a 90% confidence level [126] but later modified after several reanalyses [127, 128] to values around $70 \leq \tilde{\Lambda} \leq 700$.

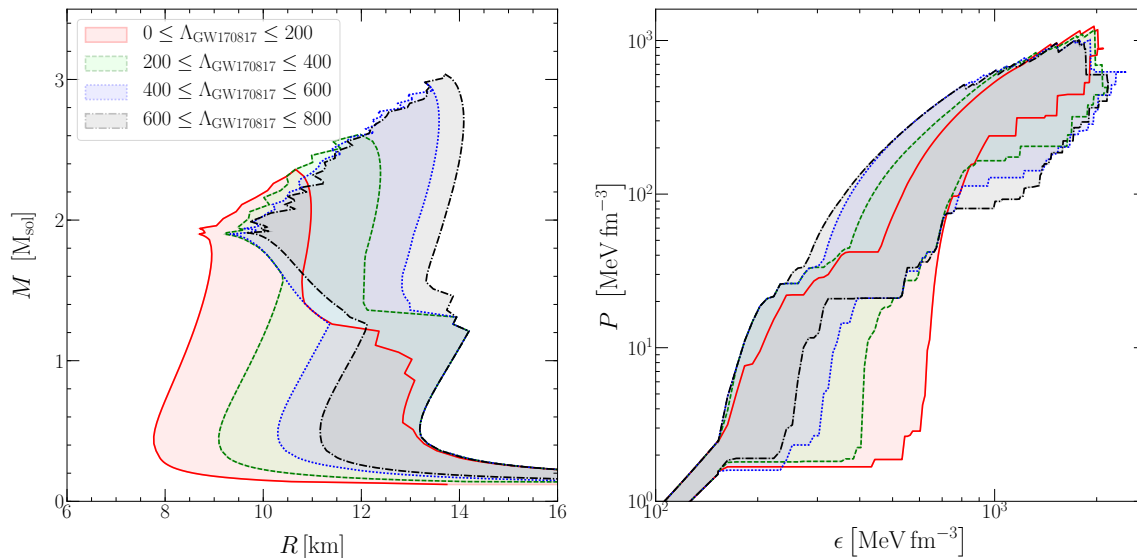


Figure 9. The MR relation and EOS using chiral EFT input up to $n_{\text{tr}} = \rho_0$, if the tidal polarizability of GW170817 could be constrained to lie in the respective ranges.

Qualitatively, neutron stars with larger radii can exhibit stronger deformations than small NS and, therefore, also have larger tidal polarizabilities. Hence, the tidal polarizability is closely related to the structure of a NS and can help to place constraints to the EOS. Using the chiral EFT results discussed in Sec. 2 up to saturation density (left panel of Fig. 6), in Fig. 9 we show the resulting MR and EOS envelopes if $\tilde{\Lambda}$ would be constrained to the 4 specified ranges, stretching from $0 \leq \tilde{\Lambda} \leq 800$. While the observation GW170817 basically allows for a total radius range of $8.4 - 13.6$ km for a typical $1.4M_{\odot}$ neutron star, we see that more precise observations in future might help to drastically constrain the radii of neutron stars and, therefore, the EOS. For example, constraining the tidal polarizability to lie in an interval with a width $\Delta\tilde{\Lambda} \approx 200$, reduces the radius uncertainty to ≈ 2 km for a typical neutron star.

4.3. Bayesian Inference: Using Neutron Star Observations to Determine the EOS

A method to directly determine the EOS from neutron-star mass and radius observations was first described in Ref. [129]. Shortly thereafter, Ref. [7] presented an alternate method using Bayesian inference. Ref. [7] also obtained the first quantitative results, obtaining uncertainties in the EOS around 30% just above the nuclear saturation density. Bayesian inference is still the tool of choice for extracting the EOS, although many works employ simple Monte Carlo methods which are identical to Bayesian results with trivial priors.

One critical question (which may be soon answered) is whether or not the EOS contains a strong phase transition: a region in the EOS where the derivative of the pressure with respect to the energy density (identical to the speed of sound) is nearly

zero. Because the pressure must be continuous in the star, a strong phase transition creates a thin region in the neutron star where the energy density increases strongly with decreasing radius. Strong phase transitions of this type can result in mass-radius curves which have multiple branches, as described in Ref. [130] and recently explored in Ref. [131].

Below, we show that multiple branches in the mass-radius curve cannot be easily handled in the Bayesian methods which have been previously used in the literature and we show how this difficulty can be fixed. The traditional method for extracting the mass-radius curve from N neutron star mass and radius determinations (each expressed in the form of a two-dimensional probability distribution $\mathcal{D}(R, M)$) is to use a likelihood function of the form

$$\mathcal{L}(\{p_j\}) = \int \prod_{i=1}^N dM_i \mathcal{D}_i[R(M_i, \{p_j\}), M_i], \quad (30)$$

where $\{p_j\}$ are the parameters of the EOS and the TOV equations are solved to obtain the function $R(M_i, \{p_j\})$. (This likelihood is analogous to Eq. (15) of Ref. [129] and Eqs. (29) and (31) of Ref. [7], but the formalism in these two works is a bit different, see Ref. [132] for an interesting discussion comparing the two works.) The critical feature of these likelihoods is that they are both expressed as integrals over the gravitational mass. It is thus clear that these likelihood functions are identically zero for horizontal mass-radius curves.

In writing Eq. (30) we specifically made a choice to parametrize the M-R curve with the gravitational mass rather than the radius. Alternatively, we could have chosen the radius instead

$$\mathcal{L}(\{p_j\}) = \int \prod_{i=1}^N dR_i \mathcal{D}_i[R_i, M(R_i, \{p_j\})], \quad (31)$$

where the TOV equations now provide the function $M(R_i, \{p_j\})$. This likelihood is not equivalent to Eq. (30); it results in different posterior distributions and, given an EOS parametrization, will be maximized at a different location in parameter space. To see this, note that Eq. (30) can be rewritten as

$$\mathcal{L}(\{p_j\}) = \int \prod_{i=1}^N dR_i \mathcal{D}_i[R_i, M(R_i, \{p_j\})] \sqrt{1 + \left(\frac{dM_i}{dR_i}\right)_{\{p_j\}}} \quad (32)$$

which is not equal Eq. (31).

Choosing either Eq. (30) or Eq. (31) is further problematic because M-R curves like those from EOSs with strong phase transitions can result in two (or even three) configurations with the same gravitational mass yet different radii. The only way to use the likelihood in Eq. (30) is to break up the integral into different parts for each branch of the M-R curve

$$\mathcal{L}(\{p_j\}) = \int_{M_0}^{M_1} \prod_{i=1}^N dM_i \mathcal{D}_i[R(M_i, \{p_j\}), M_i]$$

$$+ \int_{M_2}^{M_3} \prod_{i=1}^N dM_i \mathcal{D}_i[R(M_i, \{p_j\}), M_i] \quad (33)$$

where $M_0 < M_1$ and $M_2 < M_3$ but $M_2 < M_1$. This form of the likelihood makes the numerical evaluation of the likelihood more awkward. One possible resolution is to use the central neutron star pressure, P instead of the gravitational mass M or radius R , i.e.

$$\mathcal{L}(\{p_j\}) = \int \prod_{i=1}^N dP_i \mathcal{D}_i[R(P_i, \{p_j\}), M(P_i, \{p_j\})]. \quad (34)$$

This integral is simpler because the functions $R(P_i, \{p_j\})$ and $M(P_i, \{p_j\})$ are never multiply-valued and the pressure is continuous within the star. This form has the additional advantage that neither “horizontal” nor “vertical” mass-radius curves are arbitrarily given zero likelihood, though this choice is still part of the prior distribution. Note that choosing the central energy density, instead of the central pressure, as suggested by Eq. (14) in Ref. [8] also leads to multiple integrals as in Eq. (33) when strong phase transitions create regions where $dP/d\varepsilon = 0$.

Ref. [133] recently clarified why the ambiguity between Eqs. (30) and (31) arises. It originates in the fact that we are attempting to match a one-dimensional model curve (the size of the EOS parameter space is not important for this discussion) to a two-dimensional data set $\mathcal{D}(R, M)$. In the language of differential geometry, we are embedding the curve into the data space and the ambiguity we found above is related to the choice of how we perform this embedding. The general form requires a metric (g) to specify how distances are defined

$$\begin{aligned} \mathcal{L}(\{p_j\}) = & \int \prod_{i=1}^N d\lambda_i \mathcal{D}_i[R(\lambda_i, \{p_j\}), M_i(\lambda_i, \{p_j\})] \\ & \times \left[g_{jk} \left(\frac{dX_j}{d\lambda_i} \right)_{\{p_j\}} \left(\frac{dX_k}{d\lambda_i} \right)_{\{p_j\}} \right]. \end{aligned} \quad (35)$$

where j and k range from 1 to 2 and $X_1 \equiv M$ and $X_2 \equiv R$ and for simplicity we can assume the metric is independent of i . The ambiguity in choosing the likelihood function is now explicit in the choice of the metric, g_{jk} . In the context of Bayesian inference, this metric choice is to be regarded as part of the prior probability. Choosing $\lambda_i = P_i$ and a trivial metric $g_{jk} = \delta_{jk}$ gives Eq. (34). It is clear, however, that other choices of the metric (the elements may depend on λ or X) will give different results.

The implication, in the context of future gravitational wave observations of neutron star mergers, is that unambiguous determinations of the EOS will have to wait until sufficient data is obtained as to make the posterior distributions of quantities of interest (such as EOS parameters) are not strongly dependent on the choice of prior probability. This prior probability includes the EOS parametrization and the prior probabilities for the EOS parameters [18] as well as the prior choice of metric in Eq. (35).

5. Summary

In this paper, we have reviewed current calculations of the EOS of neutron-star matter starting from AFDMC calculations of pure neutron matter using interactions from chiral EFT. We have presented the EOS of PNM with theoretical uncertainties and explained, how to extend these PNM calculations to neutron-star conditions. We then used this to explore current theoretical uncertainties for the mass-radius relation of neutron stars.

We have then discussed how this microphysics can be connected to multimessenger observations of neutron-star mergers, using several EOS models or Bayesian inference.

Neutron-star mergers offer an ideal way to constrain the EOS of strongly interacting matter, and thus, nuclear interactions. To pin down the nuclear interaction, theorists working on a solid theoretical description of microphysics, computational astrophysicists who simulate neutron-star mergers and supernovae, and observers have to work hand-in-hand to reliably extract constraints from future merger observations.

Acknowledgments

The work of S.G. and I.T. was supported by the U.S. DOE under contract DE-AC52-06NA25396 and by the LANL LDRD program. The work of S.G. was also supported by the NUCLEI SciDAC program and by the DOE Early Career Research Program. the work of JL was supported by the Laboratory Directed Research and Development program of Los Alamos National Laboratory under project number 20190021DR. The work of XD and AWS was supported by DOE SciDAC grant de-sc0018232. The work of MA and AWS was supported by NSF grant PHY 1554876. This work was supported by the US Department of Energy through the Los Alamos National Laboratory and used resources provided by the Los Alamos National Laboratory Institutional Computing Program. Los Alamos National Laboratory is operated by Triad National Security, LLC, for the National Nuclear Security Administration of U.S. Department of Energy (Contract No. 89233218CNA000001). We also used resources provided by NERSC, which is supported by the US DOE under Contract DE-AC02-05CH11231, and by the Jülich Supercomputing Center.

Figs. 2 and 3 are open source and available at <https://github.com/awsteiner/nstar-plot>.

References

- [1] Burbidge E M, Burbidge G R, Fowler W A and Hoyle F 1957 *Rev. Mod. Phys.* **29** 547–650 URL <https://doi.org/10.1103/RevModPhys.29.547>
- [2] Cameron A G 1959 *ApJ* **130** 884 URL <https://doi.org/10.1086/146780>
- [3] Demorest P B, Pennucci T, Ransom S M, Roberts M S E and Hessels J W T 2010 *Nature* **467** 1081–1083

- [4] Antoniadis J, Freire P C C, Wex N, Tauris T M, Lynch R S, van Kerkwijk M H, Kramer M, Bassa C, Dhillon V S, Driebe T, Hessels J W T, Kaspi V M, Kondratiev V I, Langer N, Marsh T R, McLaughlin M A, Pennucci T T, Ransom S M, Stairs I H, van Leeuwen J, Verbiest J P W and Whelan D G 2013 *Science* **340** 1233232 URL <http://www.sciencemag.org/content/340/6131/1233232.abstract>
- [5] Fonseca E, Pennucci T T, Ellis J A, Stairs I H, Nice D J, Ransom S M, Demorest P B, Arzoumanian Z, Crowter K, Dolch T, Ferdman R D, Gonzalez M E, Jones G, Jones M L, Lam M T, Levin L, McLaughlin M A, Stovall K, Swiggum J K and Zhu W 2016 *ApJ* **832** 167
- [6] Ozel F, Baym G and Guver T 2010 *Phys. Rev.* **D82** 101301 URL <https://doi.org/10.1103/PhysRevD.82.101301>
- [7] Steiner A W, Lattimer J M and Brown E F 2010 *Astrophys. J.* **722** 33–54 URL <https://doi.org/10.1088/0004-637X/722/1/33>
- [8] Ozel F, Psaltis D, Guver T, Baym G, Heinke C and Guillot S 2016 *Astrophys. J.* **820** 28 URL <https://doi.org/10.3847/0004-637X/820/1/28>
- [9] Steiner A W, Heinke C O, Bogdanov S, Li C, Ho W C G, Bahramian A and Han S 2018 *Mon. Not. Roy. Astron. Soc.* **476** 421 URL <https://doi.org/10.1093/mnras/sty215>
- [10] Nättilä J, Miller M C, Steiner A W, Kajava J J E, Suleimanov V F and Poutanen J 2017 *Astron. and Astrophys.* **608** A31 URL <https://doi.org/10.1051/0004-6361/201731082>
- [11] Abbott B P, Abbott R, Abbott T D, Acernese F, Ackley K, Adams C, Adams T, Addesso P, Adhikari R X, Adya V B and et al 2017 *Physical Review Letters* **119** 161101 (*Preprint* 1710.05832)
- [12] Lonardonì D, Lovato A, Gandolfi S and Pederiva F 2015 *Phys. Rev. Lett.* **114**(9) 092301 URL <http://link.aps.org/doi/10.1103/PhysRevLett.114.092301>
- [13] Alford M G, Schmitt A, Rajagopal K and Schäfer T 2008 *Rev. Mod. Phys.* **80**(4) 1455–1515 URL <https://link.aps.org/doi/10.1103/RevModPhys.80.1455>
- [14] D’Ái A, Evans P A, Burrows D N, Kuin N P M, Kann D A, Campana S, Maselli A, Romano P, Cusumano G, La Parola V, Barthelmy S D, Beardmore A P, Cenko S B, De Pasquale M, Gehrels N, Greiner J, Kennea J A, Kloise S, Melandri A, Nousek J A, Osborne J P, Palmer D M, Sbarufatti B, Schady P, Siegel M H, Tagliaferri G, Yates R and Zane S 2016 *Mon. Not. R. Astron. Soc.* **463** 2394–2404 URL <https://doi.org/10.1093/mnras/stw2023>
- [15] Hessels J W T, Ransom S M, Stairs I H, Freire P C C, Kaspi V M and Camilo F 2006 *Science* **311** 1901–1904 URL <https://doi.org/10.1126/science.1123430>
- [16] Woods P M, Kouveliotou C, Finger M H, Göğös E, Wilson C A, Patel S K, Hurley K and Swank J H 2007 *Astrophys. J.* **654** 470 URL <https://doi.org/10.1086/507459>

- [17] Karako-Argaman C, Kaspi V M, Lynch R S, Hessels J W T, Kondratiev V I, McLaughlin M A, Ransom S M, Archibald A M, Boyles J, Jenet F A, Kaplan D L, Levin L, Lorimer D R, Madsen E C, Roberts M S E, Siemens X, Stairs I H, Stovall K, Swiggum J K and van Leeuwen J 2015 *Astrophys. J.* **809** 67 (*Preprint* 1503.05170) URL <https://doi.org/10.1088/0004-637X/809/1/67>
- [18] Steiner A W, Lattimer J M and Brown E F 2016 *Eur. Phys. J. A* **52** 18 (*Preprint* 1510.07515) URL <http://doi.org/10.1140/epja/i2016-16018-1>
- [19] Steiner A W, Gandolfi S, Fattoyev F J and Newton W G 2015 *Phys. Rev. C* **91** 015804 (*Preprint* 1403.7546) URL <https://doi.org/10.1103/PhysRevC.91.015804>
- [20] Steiner A W, Prakash M, Lattimer J M and Ellis P J 2005 *Phys. Rep.* **411** 325 (*Preprint* nucl-th/0410066) URL <http://doi.org/10.1016/j.physrep.2005.02.004>
- [21] Akmal A, Pandharipande V R and Ravenhall D G 1998 *Phys. Rev. C* **58**(3) 1804–1828
- [22] Hebeler K and Schwenk A 2010 *Phys. Rev. C* **82** 014314
- [23] Hagen G, Papenbrock T, Ekström A, Wendt K A, Baardsen G, Gandolfi S, Hjorth-Jensen M and Horowitz C J 2014 *Phys. Rev. C* **89**(1) 014319 URL <https://link.aps.org/doi/10.1103/PhysRevC.89.014319>
- [24] Sarsa A, Fantoni S, Schmidt K E and Pederiva F 2003 *Phys. Rev. C* **68** 024308
- [25] Carlson J, Morales J, Pandharipande V R and Ravenhall D G 2003 *Phys. Rev. C* **68**(2) 025802 URL <https://link.aps.org/doi/10.1103/PhysRevC.68.025802>
- [26] Schmidt K E and Fantoni S 1999 *Phys. Lett. B* **446** 99–103
- [27] Gandolfi S, Gezerlis A and Carlson J 2015 *Annu. Rev. Nucl. Part. Sci.* **65** 303–328 URL <http://dx.doi.org/10.1146/annurev-nucl-102014-021957>
- [28] Carlson J, Gandolfi S, Pederiva F, Pieper S C, Schiavilla R, Schmidt K E and Wiringa R B 2015 *Rev. Mod. Phys.* **87**(3) 1067–1118 URL <http://link.aps.org/doi/10.1103/RevModPhys.87.1067>
- [29] Pudliner B S, Pandharipande V R, Carlson J, Pieper S C and Wiringa R B 1997 *Phys. Rev. C* **56** 1720–1750 ISSN 0556-2813 URL <http://link.aps.org/doi/10.1103/PhysRevC.56.1720>
- [30] Gandolfi S, Illarionov A Y, Schmidt K E, Pederiva F and Fantoni S 2009 *Phys. Rev. C* **79**(5) 054005 URL <http://link.aps.org/doi/10.1103/PhysRevC.79.054005>
- [31] Lonardoni D, Carlson J, Gandolfi S, Lynn J E, Schmidt K E, Schwenk A and Wang X B 2018 *Phys. Rev. Lett.* **120**(12) 122502
- [32] Lonardoni D, Gandolfi S, Lynn J E, Petrie C, Carlson J, Schmidt K E and Schwenk A 2018 *Phys. Rev. C* **97**(4) 044318
- [33] Lonardoni D, Gandolfi S, Wang X B and Carlson J 2018 *Phys. Rev. C* **98**(1) 014322

- [34] Wiringa R and Pieper S 2002 *Phys. Rev. Lett.* **89** 18–21 ISSN 0031-9007 URL <http://link.aps.org/doi/10.1103/PhysRevLett.89.182501>
- [35] Wiringa R B, Stoks V G J and Schiavilla R 1995 *Phys. Rev. C* **51**(1) 38–51 URL <http://link.aps.org/doi/10.1103/PhysRevC.51.38>
- [36] Pudliner B S, Pandharipande V R, Carlson J and Wiringa R B 1995 *Phys. Rev. Lett.* **74** 4396–4399 ISSN 0031-9007 URL <http://link.aps.org/doi/10.1103/PhysRevLett.74.4396>
- [37] Gandolfi S, Carlson J and Reddy S 2012 *Phys. Rev. C* **85** 032801 ISSN 0556-2813 URL <http://link.aps.org/doi/10.1103/PhysRevC.85.032801>
- [38] Epelbaum E, Hammer H W and Meißner U G 2009 *Rev. Mod. Phys.* **81**(4) 1773–1825 URL <http://link.aps.org/doi/10.1103/RevModPhys.81.1773>
- [39] Epelbaum E, Krebs H and Meißner U G 2015 *Eur. Phys. J. A* **51** 53 URL <http://dx.doi.org/10.1140/epja/i2015-15053-8>
- [40] Melendez J A, Wesolowski S and Furnstahl R J 2017 *Phys. Rev.* **C96** 024003 (*Preprint* 1704.03308)
- [41] Gezerlis A, Tews I, Epelbaum E, Gandolfi S, Hebeler K, Nogga A and Schwenk A 2013 *Phys. Rev. Lett.* **111**(3) 032501 URL <http://link.aps.org/doi/10.1103/PhysRevLett.111.032501>
- [42] Gezerlis A, Tews I, Epelbaum E, Freunek M, Gandolfi S, Hebeler K, Nogga A and Schwenk A 2014 *Phys. Rev. C* **90** 054323
- [43] Lynn J E, Tews I, Carlson J, Gandolfi S, Gezerlis A, Schmidt K E and Schwenk A 2016 *Phys. Rev. Lett.* **116** 062501
- [44] Lonardoni D, Carlson J, Gandolfi S, Lynn J E, Schmidt K E, Schwenk A and Wang X B 2018 *Phys. Rev. Lett.* **120**(12) 122502 URL <https://link.aps.org/doi/10.1103/PhysRevLett.120.122502>
- [45] Tews I, Carlson J, Gandolfi S and Reddy S 2018 *ApJ* **860** 149 (*Preprint* 1801.01923)
- [46] Lattimer J M and Swesty F D 1991 *Nucl. Phys.* **A535** 331–376
- [47] Hempel M private communication.
- [48] Shen G private communication.
- [49] Typel S private communication.
- [50] Steiner A W and Gandolfi S 2012 *Phys. Rev. Lett.* **108** 081102 (*Preprint* 1110.4142) URL <http://doi.org/10.1103/PhysRevLett.108.081102>
- [51] Baym G, Pethick C and Sutherland P 1971 *Astrophys. J.* **170** 299–+
- [52] Negele J W and Vautherin D 1973 *Nucl. Phys. A* **207** 298–320
- [53] Read J S, Lackey B D, Owen B J and Friedman J L 2009 *Phys. Rev.* **D79** 124032 (*Preprint* 0812.2163)
- [54] Hebeler K, Lattimer J M, Pethick C J and Schwenk A 2013 *Astrophys. J.* **773** 11 (*Preprint* 1303.4662)

- [55] Steiner A W, Lattimer J M and Brown E F 2013 *Astrophys. J. Lett.* **765** 5 (*Preprint* 1205.6871)
- [56] Tews I, Carlson J, Gandolfi S and Reddy S 2018 *Astrophys. J.* **860** 149 (*Preprint* 1801.01923)
- [57] Tews I, Margueron J and Reddy S 2018 *Phys. Rev.* **C98** 045804 (*Preprint* 1804.02783)
- [58] Alford M G, Han S and Prakash M 2013 *Phys. Rev.* **D88** 083013 (*Preprint* 1302.4732)
- [59] Bedaque P and Steiner A W 2015 *Phys. Rev. Lett.* **114** 031103 (*Preprint* 1408.5116)
- [60] Tews I 2017 *Phys. Rev.* **C95** 015803 (*Preprint* 1607.06998)
- [61] Tews I, Margueron J and Reddy S 2019 (*Preprint* 1901.09874)
- [62] Burrows A and Lattimer J M 1987 *ApJ* **318** L63
- [63] Bruenn S W 1987 *Phys. Rev. Lett.* **59** 938
- [64] Hirata K, Kajita T, Koshihara M, Nakahata M and Oyama Y 1987 *Phys. Rev. Lett.* **58** 1490
- [65] Arnett W D, Bahcall J N, Kirshner R P and Woosley S E 1989 *ARA&A* **27** 629–700
- [66] Langanke K, Martinez-Pinedo G, Sampaio J M, Dean D J, Hix W R, Messer O E B, Mezzacappa A, Liebendoerfer M, Janka H T and Rampp M 2003 *Phys. Rev. Lett.* **90** 241102 (*Preprint* astro-ph/0302459) URL <https://doi.org/10.1103/PhysRevLett.90.241102>
- [67] Pagliaroli G, Vissani F, Costantini M L and Ianni A 2009 *Astroparticle Physics* **31** 163–176 (*Preprint* 0810.0466)
- [68] Abbott B P, Abbott R, Abbott T D, Acernese F, Ackley K, Adams C, Adams T, Addesso P, Adhikari R X, Adya V B and et al 2017 *ApJ* **850** L39 (*Preprint* 1710.05836)
- [69] Lattimer J M and Schramm D N 1976 *ApJ* **210** 549–567
- [70] Mochkovitch R, Hernanz M, Isern J and Martin X 1993 *Nature* **361** 236
- [71] Janka H T, Eberl T, Ruffert M and Fryer C L 1999 *ApJ* **527** L39–L42 (*Preprint* astro-ph/9908290)
- [72] Freiburghaus C, Rosswog S and Thielemann F K 1999 *ApJ* **525** L121
- [73] Lee W H and Ramirez-Ruiz E 2007 *New Journal of Physics* **9** 17 (*Preprint* astro-ph/0701874)
- [74] Nakar E 2007 *Phys. Rep.* **442** 166 (*Preprint* astro-ph/0701748)
- [75] Gehrels N, Ramirez-Ruiz E and Fox D B 2009 *ARA&A* **47** 567
- [76] Fong W and Berger E 2013 *ApJ* **776** 18 (*Preprint* 1307.0819)

- [77] Rosswog S 2015 *International Journal of Modern Physics D* **24** 1530012-52 (*Preprint* 1501.02081)
- [78] Abbott B P, Abbott R, Abbott T D, Acernese F, Ackley K, Adams C, Adams T, Addesso P, Adhikari R X, Adya V B and et al 2017 *ApJ* **848** L12 (*Preprint* 1710.05833)
- [79] Goldstein A, Veres P, Burns E, Briggs M S, Hamburg R, Kocevski D, Wilson-Hodge C A, Preece R D, Poolakkil S, Roberts O J, Hui C M, Connaughton V, Racusin J, von Kienlin A, Dal Canton T, Christensen N, Littenberg T, Siellez K, Blackburn L, Broida J, Bissaldi E, Cleveland W H, Gibby M H, Giles M M, Kippen R M, McBreen S, McEnery J, Meegan C A, Paciesas W S and Stanbro M 2017 *ApJ* **848** L14 (*Preprint* 1710.05446)
- [80] Savchenko V, Ferrigno C, Kuulkers E, Bazzano A, Bozzo E, Brandt S, Chenevez J, Courvoisier T J L, Diehl R, Domingo A, Hanlon L, Jourdain E, von Kienlin A, Laurent P, Lebrun F, Lutovinov A, Martin-Carrillo A, Mereghetti S, Natalucci L, Rodi J, Roques J P, Sunyaev R and Ubertini P 2017 *ApJ* **848** L15 (*Preprint* 1710.05449)
- [81] Cowperthwaite P S, Berger E, Villar V A, Metzger B D, Nicholl M, Chornock R, Blanchard P K, Fong W, Margutti R, Soares-Santos M, Alexander K D, Allam S, Annis J, Brout D, Brown D A, Butler R E, Chen H Y, Diehl H T, Doctor Z, Drout M R, Eftekhari T, Farr B, Finley D A, Foley R J, Frieman J A, Fryer C L, García-Bellido J, Gill M S S, Guillochon J, Herner K, Holz D E, Kasen D, Kessler R, Marriner J, Matheson T, Neilsen Jr E H, Quataert E, Palmese A, Rest A, Sako M, Scolnic D M, Smith N, Tucker D L, Williams P K G, Balbinot E, Carlin J L, Cook E R, Durret F, Li T S, Lopes P A A, Lourenço A C C, Marshall J L, Medina G E, Muir J, Muñoz R R, Sauseda M, Schlegel D J, Secco L F, Vivas A K, Wester W, Zenteno A, Zhang Y, Abbott T M C, Banerji M, Bechtol K, Benoit-Lévy A, Bertin E, Buckley-Geer E, Burke D L, Capozzi D, Carnero Rosell A, Carrasco Kind M, Castander F J, Croce M, Cunha C E, D'Andrea C B, da Costa L N, Davis C, DePoy D L, Desai S, Dietrich J P, Drlica-Wagner A, Eifler T F, Evrard A E, Fernandez E, Flaughner B, Fosalba P, Gaztanaga E, Gerdes D W, Giannantonio T, Goldstein D A, Gruen D, Gruendl R A, Gutierrez G, Honscheid K, Jain B, James D J, Jeltama T, Johnson M W G, Johnson M D, Kent S, Krause E, Kron R, Kuehn K, Nuropatkin N, Lahav O, Lima M, Lin H, Maia M A G, March M, Martini P, McMahon R G, Menanteau F, Miller C J, Miquel R, Mohr J J, Neilsen E, Nichol R C, Ogando R L C, Plazas A A, Roe N, Romer A K, Roodman A, Rykoff E S, Sanchez E, Scarpine V, Schindler R, Schubnell M, Sevilla-Noarbe I, Smith M, Smith R C, Sobreira F, Suchyta E, Swanson M E C, Tarle G, Thomas D, Thomas R C, Troxel M A, Vikram V, Walker A R, Wechsler R H, Weller J, Yanny B and Zuntz J 2017 *ApJ* **848** L17 (*Preprint* 1710.05840)
- [82] Tanvir N R, Levan A J, González-Fernández C, Korobkin O, Mandel I, Rosswog S, Hjorth J, D'Avanzo P, Fruchter A S, Fryer C L, Kangas T, Milvang-Jensen

- B, Rosetti S, Steeghs D, Wollaeger R T, Cano Z, Copperwheat C M, Covino S, D’Elia V, de Ugarte Postigo A, Evans P A, Even W P, Fairhurst S, Figuera Jaimes R, Fontes C J, Fujii Y I, Fynbo J P U, Gompertz B P, Greiner J, Hodosan G, Irwin M J, Jakobsson P, Jørgensen U G, Kann D A, Lyman J D, Malesani D, McMahon R G, Melandri A, O’Brien P T, Osborne J P, Palazzi E, Perley D A, Pian E, Piranomonte S, Rabus M, Rol E, Rowlinson A, Schulze S, Sutton P, Thöne C C, Ulaczyk K, Watson D, Wiersema K and Wijers R A M J 2017 *ApJ* **848** L27 (*Preprint* 1710.05455)
- [83] Tanaka M, Utsumi Y, Mazzali P A, Tominaga N, Yoshida M, Sekiguchi Y, Morokuma T, Motohara K, Ohta K, Kawabata K S, Abe F, Aoki K, Asakura Y, Baar S, Barway S, Bond I A, Doi M, Fujiyoshi T, Furusawa H, Honda S, Itoh Y, Kawabata M, Kawai N, Kim J H, Lee C H, Miyazaki S, Morihana K, Nagashima H, Nagayama T, Nakaoka T, Nakata F, Ohsawa R, Ohshima T, Okita H, Saito T, Sumi T, Tajitsu A, Takahashi J, Takayama M, Tamura Y, Tanaka I, Terai T, Tristram P J, Yasuda N and Zenko T 2017 *PASJ* **69** 102 (*Preprint* 1710.05850)
- [84] Coulter D A, Foley R J, Kilpatrick C D, Drout M R, Piro A L, Shappee B J, Siebert M R, Simon J D, Ulloa N, Kasen D, Madore B F, Murguía-Berthier A, Pan Y C, Prochaska J X, Ramirez-Ruiz E, Rest A and Rojas-Bravo C 2017 *Science* **358** 1556–1558 (*Preprint* 1710.05452)
- [85] Evans P A, Cenko S B, Kennea J A, Emery S W K, Kuin N P M, Korobkin O, Wollaeger R T, Fryer C L, Madsen K K, Harrison F A, Xu Y, Nakar E, Hotokezaka K, Lien A, Campana S, Oates S R, Troja E, Breeveld A A, Marshall F E, Barthelmy S D, Beardmore A P, Burrows D N, Cusumano G, D’Ai A, D’Avanzo P, D’Elia V, de Pasquale M, Even W P, Fontes C J, Forster K, Garcia J, Giommi P, Grefenstette B, Gronwall C, Hartmann D H, Heida M, Hungerford A L, Kasliwal M M, Krimm H A, Levan A J, Malesani D, Melandri A, Miyasaka H, Nousek J A, O’Brien P T, Osborne J P, Pagani C, Page K L, Palmer D M, Perri M, Pike S, Racusin J L, Rosswog S, Siegel M H, Sakamoto T, Sbarufatti B, Tagliaferri G, Tanvir N R and Tohuvavohu A 2017 *Science* **358** 1565–1570 (*Preprint* 1710.05437)
- [86] Li L X and Paczyński B 1998 *ApJ* **507** L59 (*Preprint* astro-ph/9807272)
- [87] Lippuner J and Roberts L F 2015 *ApJ* **815** 82 (*Preprint* 1508.03133)
- [88] Fernández R and Metzger B D 2016 *Annual Review of Nuclear and Particle Science* **66** annurev-nucl-102115-044819 (*Preprint* 1512.05435)
- [89] Metzger B D 2017 *Living Reviews in Relativity* **20** 3 (*Preprint* 1610.09381)
- [90] Kasen D, Metzger B, Barnes J, Quataert E and Ramirez-Ruiz E 2017 *Nature* **551** 80–84 (*Preprint* 1710.05463)
- [91] Arnould M, Goriely S and Takahashi K 2007 *Phys. Rep.* **450** 97 (*Preprint* 0705.4512)
- [92] Lippuner J, Fernández R, Roberts L F, Foucart F, Kasen D, Metzger B D and Ott C D 2017 *MNRAS* **472** 904–918 (*Preprint* 1703.06216)

- [93] Abbott B P, Abbott R, Abbott T D, Abernathy M R, Acernese F, Ackley K, Adams C, Adams T, Addesso P, Adhikari R X and et al 2018 *Living Reviews in Relativity* **21** 3 (*Preprint* 1304.0670)
- [94] Scolnic D, Kessler R, Brout D, Cowperthwaite P S, Soares-Santos M, Annis J, Herner K, Chen H Y, Sako M, Doctor Z, Butler R E, Palmese A, Diehl H T, Frieman J, Holz D E, Berger E, Chornock R, Villar V A, Nicholl M, Biswas R, Hounsell R, Foley R J, Metzger J, Rest A, García-Bellido J, Möller A, Nugent P, Abbott T M C, Abdalla F B, Allam S, Bechtol K, Benoit-Lévy A, Bertin E, Brooks D, Buckley-Geer E, Carnero Rosell A, Carrasco Kind M, Carretero J, Castander F J, Cunha C E, D'Andrea C B, da Costa L N, Davis C, Doel P, Drlica-Wagner A, Eifler T F, Flaugher B, Fosalba P, Gaztanaga E, Gerdes D W, Gruen D, Gruendl R A, Gschwend J, Gutierrez G, Hartley W G, Honscheid K, James D J, Johnson M W G, Johnson M D, Krause E, Kuehn K, Kuhlmann S, Lahav O, Li T S, Lima M, Maia M A G, March M, Marshall J L, Menanteau F, Miquel R, Neilsen E, Plazas A A, Sanchez E, Scarpine V, Schubnell M, Sevilla-Noarbe I, Smith M, Smith R C, Sobreira F, Suchyta E, Swanson M E C, Tarle G, Thomas R C, Tucker D L, Walker A R and DES Collaboration 2018 *ApJ* **852** L3 (*Preprint* 1710.05845)
- [95] Metzger B D 2017 *arXiv e-prints* (*Preprint* 1710.05931)
- [96] Rosswog S, Feindt U, Korobkin O, Wu M R, Sollerman J, Goobar A and Martinez-Pinedo G 2017 *Classical and Quantum Gravity* **34** 104001 (*Preprint* 1611.09822)
- [97] Doctor Z, Kessler R, Chen H Y, Farr B, Finley D A, Foley R J, Goldstein D A, Holz D E, Kim A G, Morganson E, Sako M, Scolnic D, Smith M, Soares-Santos M, Spinka H, Abbott T M C, Abdalla F B, Allam S, Annis J, Bechtol K, Benoit-Lévy A, Bertin E, Brooks D, Buckley-Geer E, Burke D L, Carnero Rosell A, Carrasco Kind M, Carretero J, Cunha C E, D'Andrea C B, da Costa L N, DePoy D L, Desai S, Diehl H T, Drlica-Wagner A, Eifler T F, Frieman J, García-Bellido J, Gaztanaga E, Gerdes D W, Gruendl R A, Gschwend J, Gutierrez G, James D J, Krause E, Kuehn K, Kuropatkin N, Lahav O, Li T S, Lima M, Maia M A G, March M, Marshall J L, Menanteau F, Miquel R, Neilsen E, Nichol R C, Nord B, Plazas A A, Romer A K, Sanchez E, Scarpine V, Schubnell M, Sevilla-Noarbe I, Smith R C, Sobreira F, Suchyta E, Swanson M E C, Tarle G, Walker A R, Wester W and DES Collaboration 2017 *ApJ* **837** 57 (*Preprint* 1611.08052)
- [98] Duez M D, Foucart F, Kidder L E, Ott C D and Teukolsky S A 2010 *Class. Quant. Grav.* **27** 114106 (*Preprint* 0912.3528)
- [99] Hotokezaka K, Kyutoku K, Okawa H, Shibata M and Kiuchi K 2011 *Phys. Rev. D* **83** 124008 (*Preprint* 1105.4370)
- [100] Deaton M B, Duez M D, Foucart F, O'Connor E, Ott C D, Kidder L E, Muhlberger C D, Scheel M A and Szilagyi B 2013 *ApJ* **776** 47 (*Preprint* 1304.3384)
- [101] Bauswein A, Stergioulas N and Janka H T 2014 *Phys. Rev. D* **90** 023002 (*Preprint* 1403.5301)

- [102] Palenzuela C, Liebling S L, Neilsen D, Lehner L, Caballero O L, O'Connor E and Anderson M 2015 Phys. Rev. D **92** 044045 (*Preprint* 1505.01607)
- [103] Kawaguchi K, Kyutoku K, Nakano H, Okawa H, Shibata M and Taniguchi K 2015 Phys. Rev. D **92** 024014 (*Preprint* 1506.05473)
- [104] Radice D, Galeazzi F, Lippuner J, Roberts L F, Ott C D and Rezzolla L 2016 MNRAS **460** 3255 (*Preprint* 1601.02426)
- [105] Foucart F, Desai D, Brege W, Duez M D, Kasen D, Hemberger D A, Kidder L E, Pfeiffer H P and Scheel M A 2017 *Classical and Quantum Gravity* **34** 044002 (*Preprint* 1611.01159)
- [106] Radice D, Perego A, Hotokezaka K, Fromm S A, Bernuzzi S and Roberts L F 2018 ApJ **869** 130 (*Preprint* 1809.11161)
- [107] Kyutoku K, Kiuchi K, Sekiguchi Y, Shibata M and Taniguchi K 2018 Phys. Rev. D **97** 023009 (*Preprint* 1710.00827)
- [108] Martin D, Perego A, Arcones A, Thielemann F K, Korobkin O and Rosswog S 2015 ApJ **813** 2 (*Preprint* 1506.05048)
- [109] Wanajo S, Sekiguchi Y, Nishimura N, Kiuchi K, Kyutoku K and Shibata M 2014 ApJ **789** L39 (*Preprint* 1402.7317)
- [110] Metzger B D and Fernández R 2014 MNRAS **441** 3444 (*Preprint* 1402.4803)
- [111] Sekiguchi Y, Kiuchi K, Kyutoku K and Shibata M 2015 Phys. Rev. D **91** 064059 (*Preprint* 1502.06660)
- [112] Foucart F, O'Connor E, Roberts L, Duez M D, Haas R, Kidder L E, Ott C D, Pfeiffer H P, Scheel M A and Szilagyı B 2015 Phys. Rev. D **91** 124021 (*Preprint* 1502.04146)
- [113] Goriely S, Bauswein A, Just O, Pllumbi E and Janka H T 2015 MNRAS **452** 3894–3904 (*Preprint* 1504.04377)
- [114] Foucart F, O'Connor E, Roberts L, Kidder L E, Pfeiffer H P and Scheel M A 2016 Phys. Rev. D **94** 123016 (*Preprint* 1607.07450)
- [115] Roberts L F, Lippuner J, Duez M D, Faber J A, Foucart F, Lombardi Jr J C, Ning S, Ott C D and Ponce M 2017 MNRAS **464** 3907 (*Preprint* 1601.07942)
- [116] Siegel D M and Metzger B D 2017 *ArXiv e-prints* (*Preprint* 1705.05473)
- [117] Côté B, Fryer C L, Belczynski K, Korobkin O, Chruślińska M, Vassh N, Mumpower M R, Lippuner J, Sprouse T M, Surman R and Wollaeger R 2018 ApJ **855** 99 (*Preprint* 1710.05875)
- [118] Oertel M, Hempel M, Klähn T and Typel S 2017 *Rev. Mod. Phys.* **89**(1) 015007 URL <https://link.aps.org/doi/10.1103/RevModPhys.89.015007>
- [119] Schneider A S, Roberts L F and Ott C D 2017 *Phys. Rev.* **C96** 065802 URL <https://doi.org/10.1103/PhysRevC.96.065802>
- [120] Du X, Steiner A W and Holt J W 2019 *Phys. Rev. C* **99** 025803 URL <https://doi.org/10.1103/PhysRevC.99.025803>

- [121] Horowitz C J and Schwenk A 2006 *Phys. Lett. B* **638** 153 URL <https://doi.org/10.1016/j.physletb.2006.05.055>
- [122] Kortelainen M, McDonnell J, Nazarewicz W, Olsen E, Reinhard P G, Sarich J, Schunck N, Wild S M, Davesne D, Erler J and Pastore A 2014 *Phys. Rev. C* **89** 054314 URL <https://doi.org/10.1103/PhysRevC.89.054314>
- [123] Wellenhofer C, Holt J W, Kaiser N and Weise W 2014 *Phys. Rev. C* **89** 064009 URL <https://doi.org/10.1103/PhysRevC.89.064009>
- [124] Wellenhofer C, Holt J W and Kaiser N 2015 *Phys. Rev. C* **92** 015801 URL <https://doi.org/10.1103/PhysRevC.92.015801>
- [125] Damour T and Nagar A 2009 *Phys. Rev.* **D80** 084035 (*Preprint* 0906.0096)
- [126] Abbott B P, Abbott R, Abbott T D, Acernese F, Ackley K, Adams C, Adams T, Addesso P, Adhikari R X, Adya V B, Affeldt C, Afrough M, Agarwal B, Agathos M, Agatsuma K *et al.* (LIGO Scientific Collaboration and Virgo Collaboration) 2017 *Phys. Rev. Lett.* **119**(16) 161101
- [127] De S, Finstad D, Lattimer J M, Brown D A, Berger E and Biwer C M 2018 *Phys. Rev. Lett.* **121** 091102 [Erratum: *Phys. Rev. Lett.*121,no.25,259902(2018)] (*Preprint* 1804.08583)
- [128] Abbott B P *et al.* (LIGO Scientific, Virgo) 2019 *Phys. Rev.* **X9** 011001 (*Preprint* 1805.11579)
- [129] Özel F and Psaltis D 2009 *Phys. Rev. D* **80** 103003 URL <https://doi.org/10.1103/PhysRevD.80.103003>
- [130] Alford M G, Han S and Prakash M 2013 *Phys. Rev.* **D88** 083013 URL <https://doi.org/10.1103/PhysRevD.88.083013>
- [131] Han S and Steiner A W 2018 (*Preprint* 1810.10967)
- [132] Riley T E, Raaijmakers G and Watts A L 2018 *Mon. Not. Roy. Astron. Soc.* **478** 1093–1131 URL <https://doi.org/10.1093/mnras/sty1051>
- [133] Steiner A W 2018 (*Preprint* 1802.05339)